

Supplementary Materials

Continuous control of nonlinearity phase for harmonic generations

Guixin Li^{1,2†}, Shumei Chen^{1,2†}, Nitipat Pholchai^{3,4,5}, Bernhard Reineke³, Polis Wing Han Wong⁶, Edwin Yue Bun Pun⁶, Kok Wai Cheah^{2*}, Thomas Zentgraf^{3*}, and Shuang Zhang^{1*}

¹School of Physics & Astronomy, University of Birmingham, Birmingham, B15 2TT, UK

²Department of Physics, Hong Kong Baptist University, Kowloon Tong, Hong Kong

³Department of Physics, University of Paderborn, Warburger Straße 100, D-33098 Paderborn, Germany

⁴Department of Industrial Physics and Medical Instrumentation, King Mongkut's University of Technology North Bangkok, 1518 Pibulsongkram Road, Bangkok 10800, Thailand

⁵Lasers and Optics Research Group, King Mongkut's University of Technology North Bangkok, 1518 Pibulsongkram Road, Bangkok 10800, Thailand

⁶Department of Electronic Engineering, City University of Hong Kong, 83 Tat Chee Ave, Hong Kong

*email: kwcheah@hkbu.edu.hk; thomas.zentgraf@uni-paderborn.de; s.zhang@bham.ac.uk;

1. Phase of nonlinear polarizability for nanostructures with various rotational symmetries

Our demonstrate concept of controlling the nonlinear phase is general and not confined to third harmonic generation, it can be applied to any harmonic order. In general, for the n^{th} harmonic generation, the nanoantenna can be designed to have either $(n+1)$, or $(n-1)$ fold rotational symmetry. In Supplementary Table 1, we show the phase of the nonlinear material polarization for an incident fundamental wave of circular polarization σ in terms of the rotation angle of the structure, for various rotational symmetries and various orders of harmonic generation. From the table one can see that for second harmonic generation (SHG), the antennas need to have 3-fold rotational symmetry. In this case, for a circularly polarized fundamental wave, the nonlinear phase is related to the orientation angle θ of the structure by 3θ . In addition, the generated SHG signal would be circularly polarized as well, but opposite to that of the incident fundamental wave. As another example, for 4th-harmonic generation with a C3 structure, only the nonlinear signal of the same polarization will be generated with a nonlinear phase of 3θ . Whereas with a C5 structure, only the nonlinear signal of the opposite circular polarization will be generated with a nonlinear phase of 5θ of the rotation angle. Thus, the control of nonlinearity with nanostructures of rotational symmetry is very general and not confined to THG.



| | C2 | C3 | C4 | C5 |
|-------------------------------------|-------------------|---------|---------|---------|
| 2 nd harmonic generation | | | | |
| 3 rd harmonic generation | 2θ (σ) 4θ (-σ) | 3θ (-σ) | 4θ (-σ) | |
| 4 th harmonic generation | | 3θ (σ) | | 5θ (-σ) |
| 5 th harmonic generation | 4θ (σ) 6θ (-σ) | 6θ (-σ) | 4θ (σ) | |
| 6 th harmonic generation | | | | 5θ (σ) |

Supplementary Table S1. Phase of the nonlinear polarizability for various harmonic generations and structures of different rotational symmetries and the dependents on the rotation angle θ of the structure. The incident fundamental beam is circularly polarized with helicity σ . Depending on the symmetry and harmonic order, the generated nonlinear signal either has the same helicity as the fundamental beam, or opposite, or both.

2. Calculation of the ratio between the 0th and 1st order THG in the nonlinear phase gratings

For circularly polarized light at normal incidence a third-order nonlinear material polarization (induced nonlinear dipole) with opposite circular polarization state (compared to the incident wave) is generated at each nanocross. The phase of the nonlinear dipole is controlled by the orientation angle of the nanocross with respect to the lab frame.

Based on the spatial arrangement and the rotation of the nanocrosses along the surface the nonlinear radiation from the structures will interfere in the far-field due to the different phases of the nonlinear dipoles. In our experiments we used a superlattice arrangement of the nanocrosses for generating a constructive interference into the first diffraction order. For the configuration shown in Fig. S1a, the four nanocrosses in the subset I of the superlattice have an angle difference of θ with those in subset II, therefore the phase difference between the nonlinear dipole moments in the two subsets is $4\sigma\theta$. Along the 0th diffraction order (Fig. S1b), the resulting THG signal is the sum of the contributions of all the nanocrosses, which is proportional to

$$I_0^{3\omega} \propto A^2 \left| 4 + 4e^{i4\sigma\theta} \right|^2 = 32A^2 [1 + \cos(4\theta)] \quad (1)$$

where A is the amplitude of the nonlinear dipole moment of a single nanocross. We note that the intensity for the THG signal will become zero into the 0th diffraction order when the rotation angle between the nanocrosses is $\theta=\pi/4$.

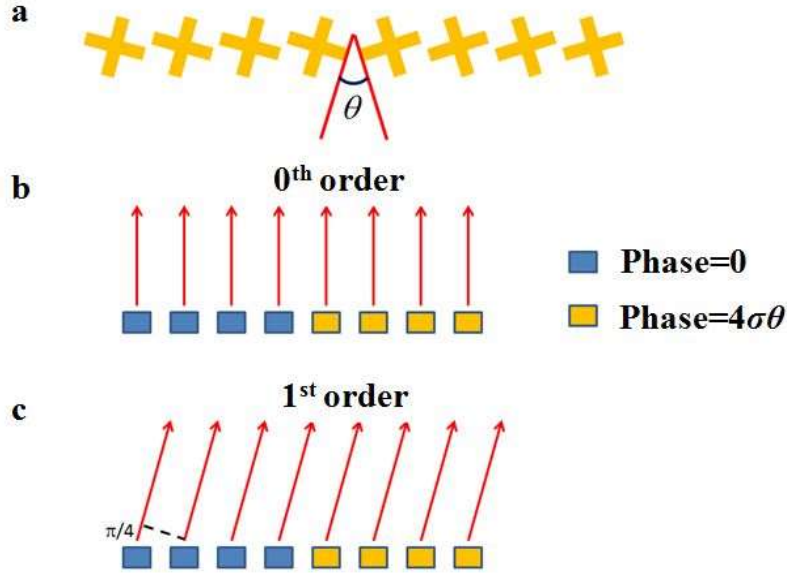


Figure S1| Schematic illustration of the formation of the diffraction orders. a, Arrangement of C4 symmetric structures along a 2D metasurface consisting of subset I and subset II in a superlattice. Each subset has four nanocrosses and the orientation angle between the nanocrosses in I and II is θ . **b**, **c**, Phase distribution of the third order nonlinear dipole and working mechanism of THG at zero or 1st diffraction orders.

On the other hand, along the 1st or -1st order, besides the $4\sigma\theta$ phase difference between the two subsets, there exists a phase step of $\pi/4$ between neighboring dipoles (for a superlattice consisting of 8 dipoles) due to the additional optical path length into the 1st or -1st order (Fig. S1c). Hence, the THG intensity into the 1st or -1st order is given by

$$I_{\pm 1}^{3\omega} \propto A^2 \left| \sum_{s=0}^3 \exp(is\pi/4) + \exp(i\pi + i4\sigma\theta) \sum_{s=0}^3 \exp(is\pi/4) \right|^2 = 4(2 + \sqrt{2})A^2 [1 - \cos(4\theta)] \quad (2)$$

The above equations show that the ratio between the intensity of the 0th diffraction order and that of the 1st or -1st order is $8[1 + \cos(4\theta)] : (2 + \sqrt{2})[1 - \cos(4\theta)]$. For a rotation angle of $\theta=\pi/8$ we obtain $\cos(4\theta)=0$ and therefore a ratio of $8 : (2 + \sqrt{2}) \approx 2.4$ for the intensities of the 1st (-1st) order compared to the 0th diffraction order.

3. Numerical simulations of THG from nanocross

To gain more insight into the circularly polarized light induced THG from PFO coated nanocrosses with four-fold (C4) symmetry, we performed numerical calculation of the third-order nonlinear polarization $\vec{P}^{3\omega}$. From the theory of nonlinear optics, it is known that $\vec{P}^{3\omega}$ is related to the tensor of third-order susceptibility, which depends on the crystal classes. As the PFO thin film is regarded as an isotropic media, the third-order polarization from the PFO film is simply given by¹

$$\vec{P}^{3\omega}(\vec{r}) = 3 \cdot \chi^{(3)} \vec{E}^\omega(\vec{r})(\vec{E}^\omega(\vec{r}) \cdot \vec{E}^\omega(\vec{r})) \quad (3)$$

where $\chi^{(3)}$ is the third-order susceptibility of PFO. $\vec{E}_j^\omega(\vec{r})$ is the electric field vector of the fundamental wave. Eq. 3 tells us that circularly polarized incident light ($\vec{E}_x = \sqrt{2}/2$, $\vec{E}_y = -i \cdot \sqrt{2}/2$, RCP) cannot generate a THG signal on bare PFO thin film. When the gold nanocross is embedded into the PFO film, the symmetry of the gold/PFO hybrid system is formed at a macroscopic level.

The nonlinear generation to the far field can be considered in two steps. First, the fundamental circularly polarized wave excites the nanostructure, leading to a certain field distribution. The nonlinear polarization radiates into far field, mediated by the plasmonic nanocross. A Green's function $\vec{G}(\vec{r}', \vec{r})$ relates a point dipole source at location \vec{r} in the nonlinear medium to the electric field at far field location \vec{r}' at frequency of 3ω . Furthermore, the reciprocity theorem states that the Green's function stays the same when source and probe can be exchanged, i.e. $G_{ij}(\vec{r}', \vec{r}) = G_{ji}(\vec{r}, \vec{r}')$. The reciprocity principle greatly simplifies the numerical evaluation of the Green's function in the way that the Green's function for third harmonic generation can be obtained by simply calculating the field distribution in the nonlinear medium when excited by a plane wave with a frequency of 3ω . While we use x, y, z as the coordinate index in the nonlinear medium, we use L (LCP) and R (RCP) for the far field location as we are only concerned about the circularly polarized state in the far field. Thus, in the tensor form, the handedness dependent Green's functions at frequency 3ω can be expressed as²:

$$G(r, r') = \begin{pmatrix} G_{xL} & G_{xR} & 0 \\ G_{yL} & G_{yR} & 0 \\ G_{zL} & G_{zR} & 0 \end{pmatrix} \text{ and } G(r', r) = \begin{pmatrix} G_{xR} & G_{yR} & G_{zR} \\ G_{xL} & G_{yL} & G_{zL} \\ 0 & 0 & 0 \end{pmatrix} \quad (4)$$

For an incident fundamental wave of left handed circular polarization, the third harmonic signal in the far field is given by:

$$\vec{E}^{3\omega}(r') = \int \vec{G}(r', r) \cdot \vec{P}^{3\omega}(r) d^3r \quad (5)$$

The integration can be rewritten as,

$$\vec{G}(r', r) \cdot \vec{P}^{3\omega}(r) = (\vec{f}_L \cdot \vec{P}) \hat{e}_L + (\vec{f}_R \cdot \vec{P}) \hat{e}_R \quad (6)$$

where $\vec{f}_L(r) = G_{xL}\hat{e}_x + G_{yL}\hat{e}_y + G_{zL}\hat{e}_z$ and $\vec{f}_R(r) = G_{xR}\hat{e}_x + G_{yR}\hat{e}_y + G_{zR}\hat{e}_z$. Thus, $(\vec{f}_L \cdot \vec{P})$ and $(\vec{f}_R \cdot \vec{P})$ represent the contribution from each local point in the nonlinear medium to the left- and right- handed circularly polarized nonlinear signal in the far field, respectively. For RCP incident fundamental light, there is no far field radiation of THG signal with the same circular polarization.

For our simulations we used for the size of unit cell 400 nm by 400 nm, the size of gold nanorod 230 nm by 60 nm, and for the thickness of gold and PFO 30 nm and 100 nm respectively. The full wave simulation software Lumerical FDTD is employed to calculate the electric field and all the elements of the Green's function in equation (5) at both fundamental and THG frequencies within one unit cell. In all the calculations, the measured dielectric constant of gold is used³. The simulations show that the nonlinear polarization is very intense around the corners of the gold nanocross if the pumping laser is at the plasmon resonant wavelength (1250 nm). In addition, the nonlinear polarization also has a C4 symmetry distribution. From the calculated results, we found that the RCP/LCP polarized fundamental waves only generate LCP/RCP polarized THG from the nanocross. In Fig. S2a and Fig. S3a, we present the two dimensional plot of the amplitude and phase of $(\vec{f}_L \cdot \vec{P})$ and $(\vec{f}_R \cdot \vec{P})$ (local contribution to the LCP/RCP nonlinear signal in the far-field).

The amplitude distribution shown in Fig. S2a and Fig. S3a show that the contribution to far-field nonlinear radiation is strongly confined to the tips of the nanocross, which is well expected. From the phase distribution shown in Fig. S2b and Fig. S3b, one can see that the nonlinear phase is strongly dependent on the orientation angle of the nanocross. To better visualize the dependence of the nonlinear phase over different orientations, we subtract a phase of $4\sigma\theta$ from the phase distribution of each plot in Fig. S2b and Fig. S3b (where θ is the orientation angle of the nanocross), and we obtain exactly the same phase for all the orientations, as shown in Fig. S2c and Fig. S3c. This verifies that the phase of the nonlinearity is related to the orientation angle by a factor of ± 4 , agreeing with our analytical analysis based on coordinate transformation (Eq. 6 in the main text).

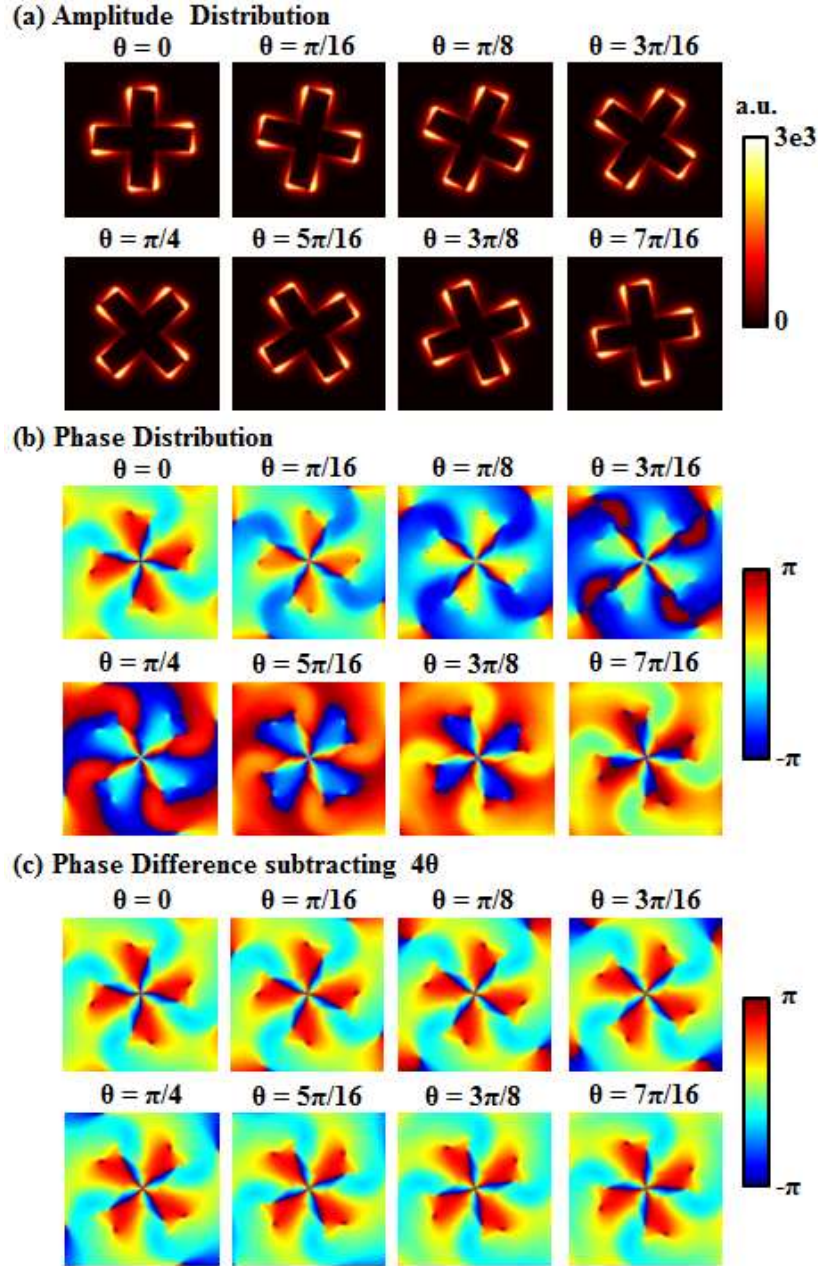


Figure S2| 2D distribution of $(\vec{f}_L \cdot \vec{P})$, which represents the local contribution to the LCP nonlinear signal in the far field. a, The amplitude distribution showing the contribution is confined to the tips of the nanocrosses. **b,** The phase distribution shows the strong dependence of the nonlinear phase over the orientation angle. **c,** Subtracting a uniform phase of 4θ from each figure in **b** giving rise to the same phase distribution. This verifies that the nonlinear phase is related to the orientation angle of the structure by a factor of 4.

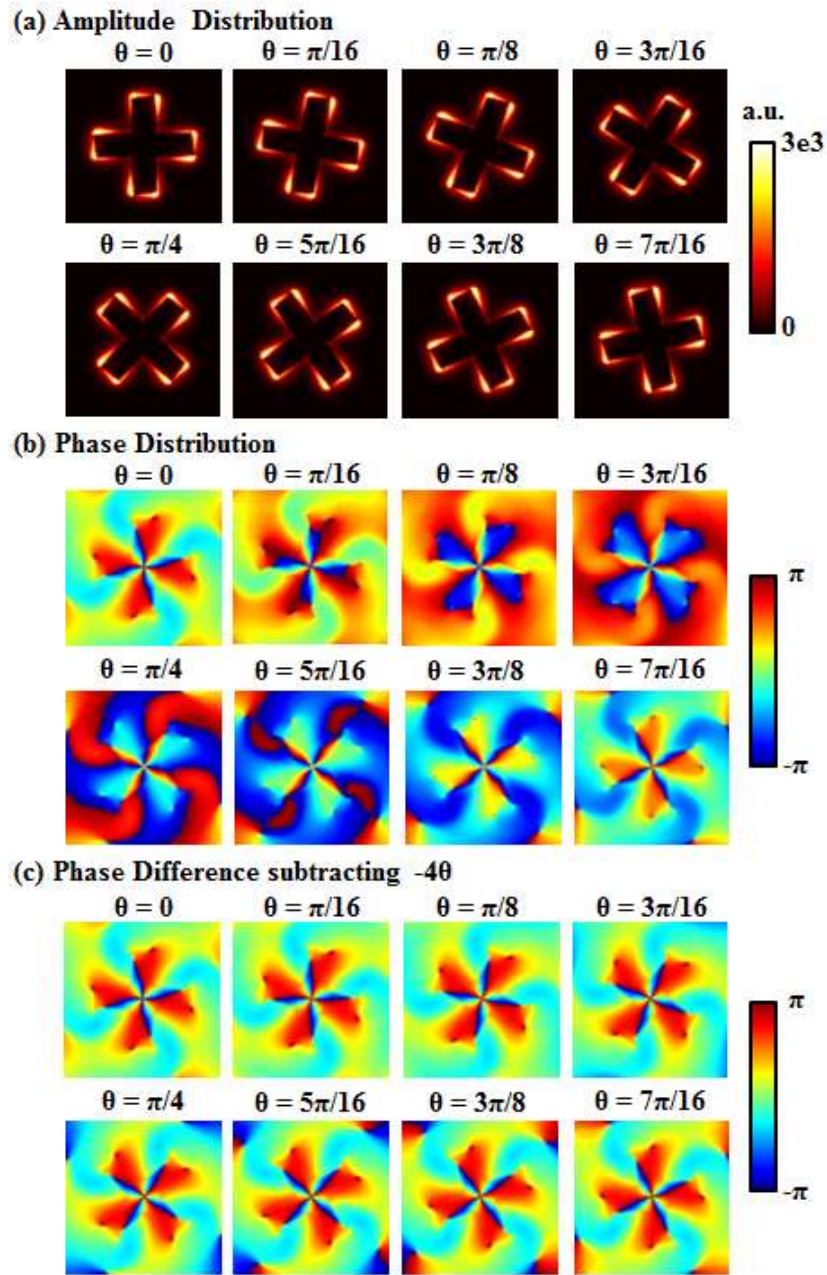


Figure S3| 2D distribution of $(\vec{f}_r \cdot \vec{P})$, which represents the local contribution to the RCP nonlinear signal in the far field. a, The amplitude distribution showing the contribution is confined to the tips of the nanocrosses. **b**, The phase distribution shows the strong dependence of the nonlinear phase over the orientation angle. **c**, Subtracting a uniform phase of -4θ from each figure in **b** giving rise to the same phase distribution. This verifies that the nonlinear phase is related to the orientation angle of the structure by a factor of -4 .

4. Diffraction of second harmonic generation (SHG) with a metasurface consisting of C3 nanostructures

In addition to the measurements on THG from the C4 symmetry structures we performed additional measurements of second harmonic generation (SHG) for a metasurface consisting of C3 rotational symmetric structures (Fig. S4). For the measurements we fabricated pattern with nanoantennas of 3-fold rotational symmetry by electron beam lithography. The nanoantennas have a period of 400 nm in both x- and y-direction. Along the x-direction the nanoantennas are rotated in steps 15° to generate a phase gradient in the second-order polarization. The resonance wavelength of the fabricated C3 structures was around 1070 nm and therefore slightly short than for the C4 geometry. Therefore, we used as fundamental wavelength 1100 nm. The measurements shown in Fig. S4c correspond to the same situation as shown in Fig. 4 of the main text but for SHG instead of THG. Due to the C3 rotational symmetry of the structure, generation of SHG signal with the same polarization is forbidden, whereas for the cross-polarized SHG signal (RCP-LCP and LCP-RCP) the diffraction angle is determined by the gradient of the orientation of the C3 nanostructures. Our measurements verify that the concept works also for other nonlinear processes despite the THG process.

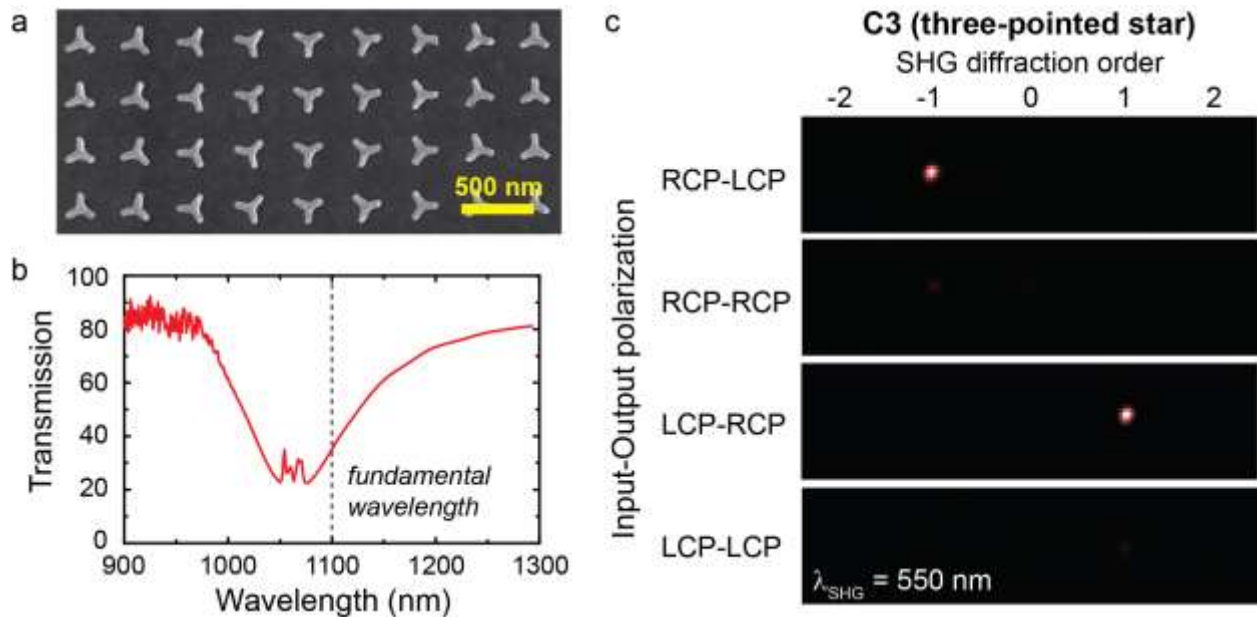


Figure S4| SHG measurement from a metasurface with nanoantennas of C3 rotational symmetry. **a**, Scanning electron microscopy image of the metasurface. The structures are rotated along the x-direction by an angle of 15° , generating a linear phase gradient along the surface. **b**, Transmission spectrum of the pattern showing the resonance at 1070 nm. The small peaks around the resonance wavelength are artifacts of our supercontinuum light source. **c**, Measured SHG signal for a fundamental beam at 1100 nm in dependence on the polarization state. The diffraction of the SHG signal appears under a diffraction angle of $\pm 9.75^\circ$ (± 1 order) in correspondence with the designed phase gradient.

References:

1. Boyd, R. W. Nonlinear Optics, Academic Press, San Diego, USA 2008.
2. Novotny, L. & Hecht, B. Principle of Nano Optics, (Cambridge University, 2006).
3. Palik, E. D. Handbook of Optical Constants of Solids (Academic, 1985).